



## Toward hydrophobicity without surface functionalization through organosilane sol gel coatings on nano-roughed aluminum substrate

S. Shadmani, M. Khodaei\*

Faculty of Materials Science and Engineering, K. N. Toosi University of Technology, Tehran, Iran.

Received: 15 June 2020; Accepted: 8 October 2020

\* Corresponding author email: [khodaei@kntu.ac.ir](mailto:khodaei@kntu.ac.ir)

### ABSTRACT

Hydrophobic and superhydrophobic coatings can be fabricated through the traditional two-step method, including fabrication of hierarchical micro and nanoscale roughness along with surface modification using low energy materials like fatty acids and fluoropolymers. Using a low energy material is not suitable due to its weak chemical bonding to the surface, and also, some of the used materials are toxic. Herein, a novel method has been introduced to fabricate the hydrophobic coating using the Wenzel wetting model. The aluminum substrate was chemically etched to create the nano-roughed surface structure and subsequent silane-based coatings can lead to increase the water contact angle without using any surface functionalization with low energy materials. In addition to that, two type of silane-based sol-gel coatings (TEOS and TEOS/GPTMS) have been used to investigate the benefits of hybrid organosilane sol-gel coating. The results indicated that the increasing in the surface roughness of silane-based coatings using chemical etching of the substrate leads to increase the water contact angle to hydrophobic state, which is supported by the Wenzel wetting model. The corrosion mitigation behavior of silane-based coatings on different substrate (bare and etched aluminum) has been studied in details.

**Keywords:** *Hydrophobicity, one step hydrophobic coating, hybrid sol-gel coating, organosilane, nano-roughed aluminum.*

### 1. Introduction

Hydrophobicity is a unique behavior of surfaces and coatings against water, which was first observed in nature. A hydrophobic surface has a water contact angle (WCA) between 90° to 150°. Higher WCA values are superhydrophobic, and lower are hydrophilic surfaces. Most of the superhydrophobic coatings are fabricated in the same way utilizing different materials or methods. A hierarchical micro and nanoscale roughness is first made on the surface, and then a low surface energy material is coated on top to reduce surface energy to achieve superhydrophobicity [1]. The low surface energy top coat usually consists of

fatty acid, fluoro alkylsilane, or similar material that does not have enough mechanical stability or adhesion to the substrate. That is the main reason that superhydrophobic coatings do not have enough mechanical stability [2]. Hydrophobic coatings have high corrosion resistance [3], foul-release capabilities [4], and can be used on surfaces like solar cells that are important to get cleaned easily [5].

Several wetting models have been defined to calculate contact angle on the surface [6-7]. The first wetting model is Young's equation that was just mentioned. This model does not consider surface roughness of the solid surface. Below the Young's

equation is shown (eq. 1).

$$\cos\theta = \frac{\gamma_{SG} - \gamma_{SL}}{\gamma_{LG}} \quad (1)$$

In this equation  $\theta$  is contact angle and  $\gamma_{SG}$ ,  $\gamma_{SL}$  and  $\gamma_{LG}$  are respectively surface free energy of solid/gas, solid/liquid, and liquid/gas interface.

It is evident that in most cases, the surface is not smooth, so Young's equation is not able to calculate the contact angle properly, so the Wenzel equation was introduced. In this equation, it is considered that the surface wetting occurs uniformly, and the equation is shown below (eq. 2) [7]:

$$\cos\theta_w = r\cos\theta \quad (2)$$

In this equation  $\theta_w$  is the Wenzel contact angle,  $\theta$  is Young's contact angle and  $r$  represents the surface roughness factor that is equal to the ratio of real surface to apparent surface.

As mentioned before, wetting is considered to be uniform in Wenzel's equation, or in other words, it is considered that water went through all surface cavities, and there is no dry part. On the other hand, there is another wetting model which considers that the wetting is not uniform and air packets do not let water to get into the surface cavities. In this case, water is in contact with solid and air packets and water contact angle with air is equal to  $180^\circ$ . The model is called the Cassie-Baxter, and the equation is shown below [7]:

$$\cos\theta_{CB} = f_1 * \cos\theta_1 + f_2 * \cos\theta_2 \quad (3)$$

$$\cos\theta_{CB} = f_1 * \cos\theta_0 + f_2 * \cos(\pi) \quad (4)$$

$$\cos\theta_{CB} = f_1 * \cos\theta - f_2 \quad (5)$$

$$\cos\theta_{CB} = f_1 * (\cos\theta + 1) - 1 \quad (6)$$

In the above equations  $\theta_{CB}$  is the Cassie-Baxter contact angle,  $f_1$  is the ratio of the area that liquid is in contact with solid and  $f_2$  is that ratio of the area that liquid is in contact with air packets made or trapped air inside the surface cavities.

As mentioned before, superhydrophobic coatings are not stable enough to be used in industries, and their unique behavior against water cannot be used properly. In addition to that, some of the low energy materials used in the superhydrophobic coatings to functionalize the surface are toxic and harmful to humans and nature. A different approach is taken in this article. Instead of making a superhydrophobic coating using toxic and unstable low energy material on top to functionalize coating to achieve superhydrophobicity, a sol-gel coating was used to

achieve stable hydrophobic properties. Two types of sol-gel coating were fabricated and dip-coated on the substrate. Also, a unique chemical reactive chemical etching method was used to increase the final coating's surface roughness.

There are various methods to achieve hydrophobic coating on a surface such as lithography [8], templating [9], chemical etching [10], chemical vapor deposition [11], layer by layer deposition [12], colloidal aggregation and assembling [13], electrospinning [14] and electrospraying [15], etc. Among these methods, the sol-gel process guarantees a uniform, low-cost coating with acceptable mechanical properties.

The sol-gel method is economical, versatile and has various applications like fabrication of protective films, porous films, high-temperature superconductors, etc. The sol-gel method has been used to fabricate wear-resistant coatings. The coating can be applied on metals like carbon steel, stainless steel and marine, and biotechnology industries can use this kind of coating [16]. The sol-gel coating can be applied on the surface by various methods like dip coating, spin coating, spraying, etc.

Different methods can be used to deposit a sol-gel coating on a metal substrate. The most common methods to deposit the coating are spin coating and dip coating. However, spray coating and electrodeposition have been being used recently. Spin coating and dip coating process can only be used to deposit coating on a smooth surface and they cannot be used to coat complex surfaces. The next step after deposition is drying and the temperature can be up to  $900^\circ\text{C}$ . However, for a hybrid organic-inorganic sol-gel coating, the temperature needed is about  $200^\circ\text{C}$ , which is an advantage for hybrid coatings. The heating rate during the curing is important and a lower heating rate will result in a denser coating. An increase in curing temperature for silica-based sol-gel coating will increase the chance of crack formation due to high stress during curing [17].

Inorganic oxides sol-gel coatings can be used to deposit on metal substrates, but they have two critical problems that have a negative effect on their corrosion and wear resistance. These problems are mentioned below:

1- These inorganic oxide films are brittle and achieving thickness higher than  $1\mu\text{m}$  without crack formation is very hard.

2- In order to achieve desired properties, the

coating needs to be cured at a high temperature, usually between 400°C to 900°C.

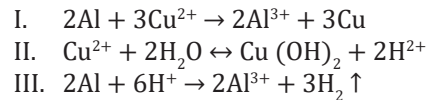
In order to overcome these problems, many approaches have been considered and tried until the organic-inorganic sol-gel coatings (hybrid sol-gel coatings) were introduced and draw much attention from scientists [18].

The hybrid sol-gel system has many advantages such as high wear resistance, excellent adhesion to the substrate, etc. These advantages resulted in the development of organic-inorganic systems called Ormocers which is referred to organically modified ceramics. These coatings consist of high inorganic materials (40%wt to 95%wt) and low organic materials (5%wt to 60%wt). The inorganic part is usually silica, which will be changed into alkoxy silanes during the sol-gel process. As mentioned before, these kinds of materials have a combination of polymer and ceramic properties and can be produced at a low temperature. Inorganic compounds increase the durability, scratch resistance and adhesion to the metal substrate while organic materials increase density, flexibility [19].

This study aimed to achieve hydrophobicity using TEOS and TEOS/GPTMS hybrid sol-gel coatings without surface functionalization. The benefits of using a hybrid sol-gel coating were also studied. Reactive chemical etching was used to modify surface roughness and increase WCA. On the other hand, the absence of surface functionalization with low energy materials will lead to stable hydrophobic properties. The main reason to avoid low energy materials is that they do not have proper mechanical stability and also in most cases, they are toxic or harmful for humans.

Reactive chemical etching is a method used to increase surface roughness on the Aluminum surface. During this process, the Aluminum plate is immersed into the CuCl<sub>2</sub> solution, the chemical substitution starts and Copper ions react with Aluminum element on the surface and aluminum chloride will be made by this reaction and as a result Copper element will deposit on the

surface. Aluminum corrosion potential is lower than Copper, so when Copper deposits on the surface of the Aluminum, a galvanic reaction will occur, and reaction speed will be increased. This reaction is exothermic and produces a lot of heat. In addition to this, the Copper on the surface reacts with solution water and Hydrogen ions will be produced, which will make the solution acidic and be able to remove Aluminum from the substrate. When the Hydrogen ions react with the Aluminum on the surface of the sample, then a small hydrogen bubble will be made on the surface, so during that time, the Copper ions cannot affect that part of the sample so as a result, the corrosion will not be uniform. That will be beneficial to achieve hierarchical micro and nanoscale roughness. Below the reactions are mentioned.



The aluminum plate is a polycrystalline metal that has grain boundaries and dislocations. These places are ideal for corrosion and chemical substitution, so immediately after immersion of Al plate into the CuCl<sub>2</sub> solution, the reaction will take place in these places, and as a result, rectangular planes and nanoscale steps will be formed on the surface [10].

**2. Materials and Method**

**2.1. Materials**

The descriptions of samples are shown in Table 1. Commercially available Al plate (AA1050) was used as a substrate. Tetraethyl orthosilicate (Si(OC<sub>2</sub>H<sub>5</sub>)<sub>4</sub>, TEOS, Merck), 3Glycidyloxypropyltrimethoxysilane (C<sub>9</sub>H<sub>20</sub>O<sub>5</sub>Si, GPTMS, Sigma-Aldrich), 1H,1H,2H,2H-Perfluorodecyltriethoxysilane (C<sub>16</sub>H<sub>19</sub>F<sub>17</sub>O<sub>3</sub>Si, FAS-17, Sigma-Aldrich), Nitric acid 65% (HNO<sub>3</sub>, Merck), Ethyl alcohol (Merck), Acetone, CuCl<sub>2</sub> (Dr. Mojallali Co., Iran) were used as received in this work.

Table 1- Sample description at a glance

#	Sample name	Coating	Substrate
1	Al	-	
2	Al-T	TEOS sol-gel coating	Bare Al
3	Al-TG	TEOS/GPTMS hybrid sol-gel coating	
4	Etch	-	
5	E-T	TEOS sol-gel coating	Chemically etched Al
6	E-TG	TEOS/GPTMS hybrid sol-gel coating	

## 2.2. Sample preparation

Al plates were cut into 20 mm × 20 mm pieces and were sequentially polished with sandpapers of #400 to #1200 along the vertical and horizontal directions alternately to remove the native oxide layer of Al surfaces. Then the pieces were washed in acetone and deionized water sequentially for 10 min using the ultrasonic bath. The cleaned Al coupons were simply immersed in a 1M CuCl<sub>2</sub> aqueous solution at room temperature for 60 seconds. Since the etching of surface can be completed after 10s of reactive chemical reaction of Al and CuCl<sub>2</sub> [10], the samples of this work have been subjected to etching for 60s in this work to ensure the complete etching. After that, all samples were rinsed and washed with deionized water in an ultrasonic bath for 10 min to get rid of the deposited Cu layer. Then the pieces were dried in the oven at 70 °C for 30 min.

TEOS and TEOS/GPTMS hybrid sols were prepared through subsequently dropwise adding of precursors to a 0.05M HNO<sub>3</sub> aqueous solution followed by stirring until clear sol was achieved. The GPTMS/TEOS molar ratio was 3/7. The ratio of the TEOS and GPTMS precursors and other parameters (curing temperature, withdraw speed, drying temperature, etc.) have been optimized in another study using the design of experiment method [20]. The sol was left at room temperature for 48 h for the aging process and then used for coating. Al coupons were coated by one step dip-coating process with an immersion time of 2 min, and a withdraw rate of 180 mm/s. After that, the samples were dried at 60°C and cured at 130°C for 90 min. The name and preparation process of the samples are given in table 1.

## 2.3. Characterization

An optical contact-angle goniometer (Model CAG-10, Jikan company, Iran) was used to measure the water contact angles (WCA) and contact angles hysteresis (WCAH) at room temperature. The WCA was reported as an average of WCA of five different spots on each specimen. WCAH was measured by adding and subtracting the liquid to the droplet water (variations on the sessile-drop method), which is based on the growth/shrinkage of a sessile drop. The volume of the droplet gradually increases by adding water to the drop, causing the contact line to advance (advancing WCA), and by subtracting water from the drop, the droplet starts to retract/recede as a result of the

decrease in volume (receding WCA). The WCAH can be defined by the difference of the maximum advancing WCA and the minimum receding WCA.

The surface morphology of samples was observed by field emission scanning electron microscope (FESEM) TESCAN-MIRA3 and atomic force microscope (AFM) DME-SPM-C26. Potentiodynamic polarization curve measurement, as well as electrochemical impedance spectroscopy (EIS), has been performed using Ivium CompactStat at room temperature to determine the corrosion behavior of samples. The measurements were done in a three-electrode system using a flat cell containing the 3.5 wt.% NaCl solution; in which a saturated calomel electrode (SCE), a platinum electrode, and the samples (1cm<sup>2</sup> exposed area) were used as the reference, the counter, and the working electrode, respectively. For the potentiodynamic polarization experiments, the open circuit potential (OCP) of immersed samples in the salt solution was scanned from -250 mV to -250mV with a sweep rate of 10 mV/s. The corrosion current density ( $J_{\text{corr}}$ ), corrosion potential ( $E_{\text{corr}}$ ), and polarization resistance ( $R_p$ ) of the samples were obtained from Tafel extrapolation of polarization curves using Iviumsoft software. The EIS measurements were performed at OCP in the frequency range from 10 MHz to 10 kHz by a sinusoidal wave with perturbation of 10 mV.

## 3. Result and discussion

### 3.1. Evaluation of wetting behavior

Surface energy and roughness are two main parameters affecting the wetting behavior of a coating. For both TEOS and TEOS/GPTMS coatings, the surface energy is in a similar range and the roughness will make a considerable change in water contact angle. The WCA for Al bare sample is about 60°, and the deposition of TEOS and TEOS/GPTMS coatings increased it to about 63° and 67°, respectively which is in the same range. The reason for the same increase in WCA is the close surface energy of TEOS and TEOS/GTPMS hybrid sol-gel coating. This project aims to investigate how one can increase WCA and achieve hydrophobicity without surface functionalization. According to the Wenzel wetting model, in order to increase WCA, surface roughness has to increase. A novel wet chemical etching method was performed before coating deposition to make a hierarchical roughness on the substrate. The WCA for etched Al substrate without sol-gel coating (Etch sample)

was 0°. The new surface morphology affected the coating microstructure and increased WCA for both coatings. According to Fig. 1, WCA increased to 106° and 118°, respectively for E-T and E-TG samples. The contact angle hysteresis for all coated samples was in the range of 28° to 35°, which indicates high adhesion of water droplet to the surface.

These results indicate that the TEOS/GPTMS sol-gel coating has a slightly higher (about 6%) WCA intrinsically, probably due to the presence of GPTMS organic chains. Additionally, it is evident that the coating combination, in this case, does not have a significant effect on the wettability of the coating. On the other hand, surface roughness produced by chemical etching of the substrate before coating deposition has a very high positive effect on increasing the coating WCA. For TEOS based sol-gel coating, the introduced surface roughness increased the WCA from 63° to 106°, and for the TEOS/GPTMS sol-gel coating from 67° to 118°.

As mentioned, in this study, the combination of coating has led to a 6% increase in WCA of the coating. On the other hand, surface roughness has led to an average 70% increase in WCA values, which has changed the wetting behavior of coatings from hydrophilic to hydrophobic. That increase in WCA of the coating is not achieved by use of any low surface energy treatment. According to the Wenzel wetting model, there is a relation between surface roughness and WCA. An increase in surface roughness by chemical etching before deposition of the coating while the coating does not cover all the micro and nanoscaled roughness and following the protrusions and bumps caused the increase in WCA. This increase in WCA by modifying surface roughness is capable of increasing the WCA to the hydrophobic region, and achieving superhydrophobicity without low surface energy and hierarchical micro and nanoscale roughness at the same time is not possible. This study aimed to achieve hydrophobicity without surface functionalization due to its instability.

### 3.2. Coating microstructure and morphology

To investigate the effect wet chemical etching method and further understand coating behavior, electrochemical impedance spectroscopy and polarization analysis was performed. The results clarified considerable results.

Before discussing the corrosion behavior

of samples, it is necessary to study the coating microstructure further. As shown in Fig. 2a cross-cut was done on Al-T and Al-TG samples to evaluate coating adherence to substrate in which, as expected, the hybrid coating has lower shrinkage and a robust uniform coating is fabricated on the substrate. According to the ASTM standard for the cross-cut test, the Al-TG was 5B with intact squares, while for Al-T, it was 4B. This lower mechanical stability is due to shrinkage and crack formation during the curing of Al-T in comparison with Al-TG.

As shown in Fig. 2b, in order to compare corrosion behavior of coatings deposited on bare Al and chemically etched Aluminum, coatings thicknesses were measured. They were 16µm and 4µm for coatings deposited on Al and chemically etched Al, respectively.

Due to the significant difference (about four times) between coatings thicknesses on Al and chemically etched Al substrates, the corrosion behavior of these two types of samples should be considered separately so that the effect of adding GPTMS to the sol-gel coating on corrosion behavior can be investigated.

As shown in Fig. 1, WCA increased by using chemical etching techniques before coating deposition. According to the Wenzel wetting model, an increase in surface roughness or, in other words, considering the surface roughness in

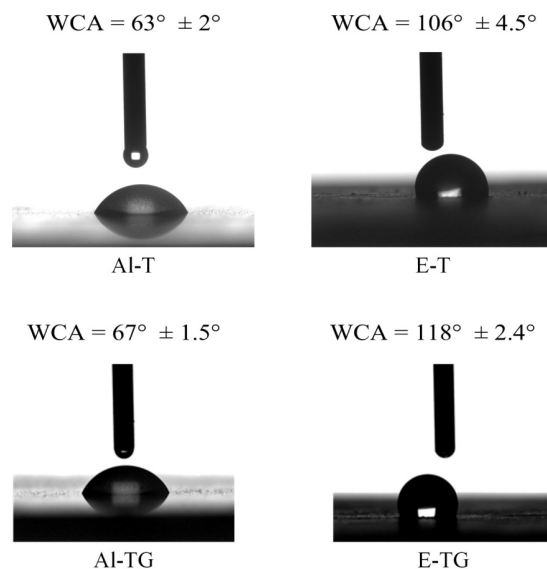


Fig. 1- WCA measurement results of Al-T, Al-TG, E-T, and E-TG samples, indicating the effect of coating combination and surface roughness on the wetting behavior of coating using 5-7 µl of deionized water.

calculations, will lead to an increase in WCA. In Fig. 3 surface morphology of Etch, E-T and E-TG are shown through FESEM images. A comparison of the surface morphology of the aforementioned samples indicates two main points. First, wet chemical etching used in this study, have caused a hierarchical micro and nanoscale roughness to be formed on the substrate before coating deposition. The second point is that both TEOS and TEOS/GPTMS hybrid coatings have followed the hierarchical surface structure; this can also be seen in Fig. 2b from the cross-section of the coatings.

In order to further study, the surface roughness and morphology of coatings deposited on chemically etched samples, Atomic force microscopy was used. In Fig. 4 AFM images of Etch, E-T, and E-TG are shown.

In table 2, the arithmetic roughness average of the surface ( $R_a$ ) and the root mean square of the surface roughness ( $R_q$ ) as two main roughness evaluation parameters are calculated from AFM. The results indicate that the E-T sample has the highest surface roughness due to the shrinkage of the coating, and possible microcrack formation on top is the reason for this observation. On the other hand, the addition of GPTMS to the coating will increase coating viscosity. As a result, during dip coating and curing, the coating will cover some of the substrate hierarchical structure, and E-TG has

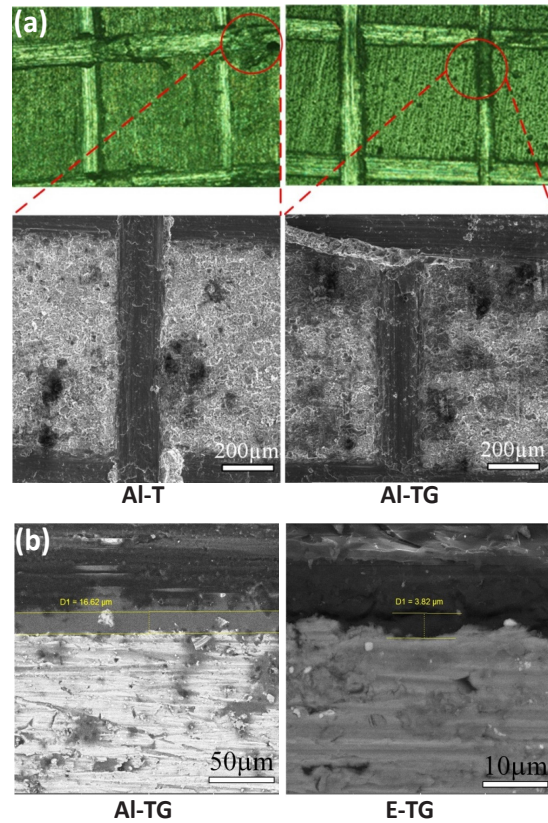


Fig. 2- (a) Optical microscope and FESEM images of Al-T and Al-TG samples after cross-cut test, (b) FESEM image of Al-TG and E-TG coatings cross-section.

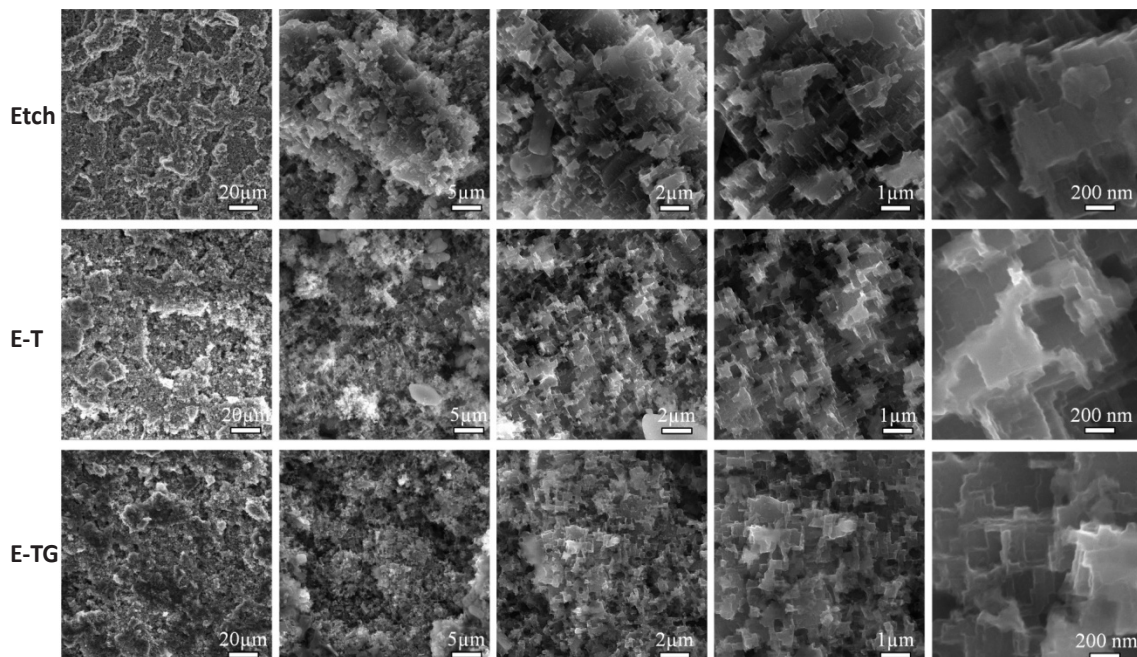


Fig. 3- FESEM images of Etch, E-T, and E-TG in various magnification indicating the surfaces micro and nanostructures.

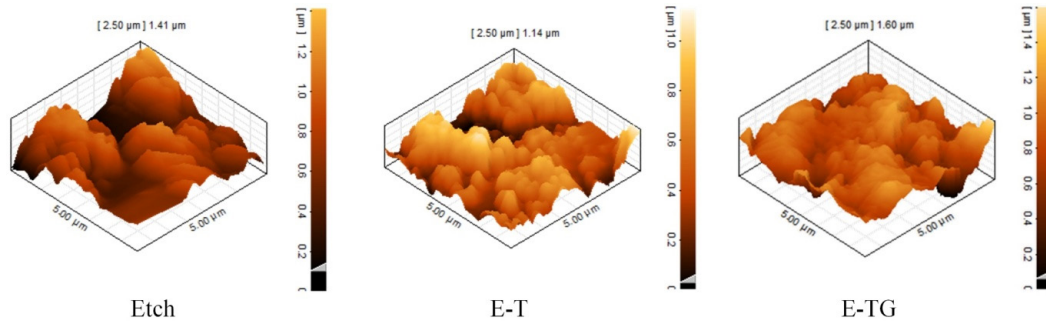


Fig. 4- AFM images of surface topography of Etch, E-T and E-TG samples at a 5x5µm area.

Table 2-  $R_a$  and  $R_q$  measurements from AFM analysis of surface morphology

Sample name	$R_a$ (nm)	$R_q$ (nm)
E	$159 \pm 19$	$195 \pm 23$
E-T	$163 \pm 7$	$201 \pm 8$
E-TG	$127 \pm 5$	$163 \pm 6$

the lowest roughness. On the other hand, coating uniformity and lack of crack formation on the coating during curing has led to higher WCA in comparison with E and E-T.

By considering the FESEM and AFM images, it is evident that the sol-gel coating did not hinder the effect of substrate micro and nanoscaled protrusions and bumps on the chemically etched substrate. That has led to a 70% increase in WCA value for E-T and E-TG samples in comparison to Al-T and Al-TG. Adding GPTMS to the sol-gel coating has led to a more uniform coating causing a decrease in surface roughness due to its proper coverage of the substrate. Furthermore, WCA results shown in Fig. 1 indicated that a combination of higher wettability of the hybrid sol-gel coating and uniformly following the substrate micro and nanostructure on the chemically etched substrate has led to high WCA (about 118°) and hydrophobicity without any surface functionalization.

### 3.3. Corrosion behavior

Coating characterizations showed that both TEOS and TEOS/GPTMS hybrid coatings have lower thicknesses on the chemically etched substrate in comparison to bare Al substrate. The coating thickness on the chemically etched substrate decrease was up to 4 times in comparison with the coating deposited on the Al substrate. A decrease in coating thickness on etched samples (E-T and E-TG) will lead to a decrease in corrosion resistance. On the other hand, an increase in WCA

should lead to increased corrosion resistance due to the blocking the corrosive ions penetration to the coating. This interaction between the positive effect of hydrophobicity and the negative effect of coating thickness on corrosion resistance should be considered while studying electrochemical impedance spectroscopy and polarization. In addition to that, high WCA in range of hydrophobicity is not always beneficial to corrosion resistance because some hydrophobic surfaces have high contact angle hysteresis and sliding angle, which will cause water droplets to adhere to coating's surface and penetrate. In other words, Al, Al-T, and Al-TG cannot be compared with Etch, E-T, and E-TG due to coating thickness and wetting behavior deference. In Fig. 5 results of EIS and Polarization tests for Al, Al-T and Al-TG are reported.

Al and Al-T showed similar corrosion resistance. That is due to inadequate coverage of the surface by TEOS sol-gel coating. The cracks formed on the coating and low viscosity of the coating will lead to weak protection from the substrate. On the other hand, the Al-TG has higher corrosion resistance due to uniform coating deposition. This increase in corrosion resistance is not only due to uniformity of the coating but also due to the presence of GPTMS in the hybrid sol-gel coating that minimizes crack formation and shrinkage during curing. That proves that using GPTMS can drastically improve coating corrosion resistance.

To compare corrosion current density, Tafel

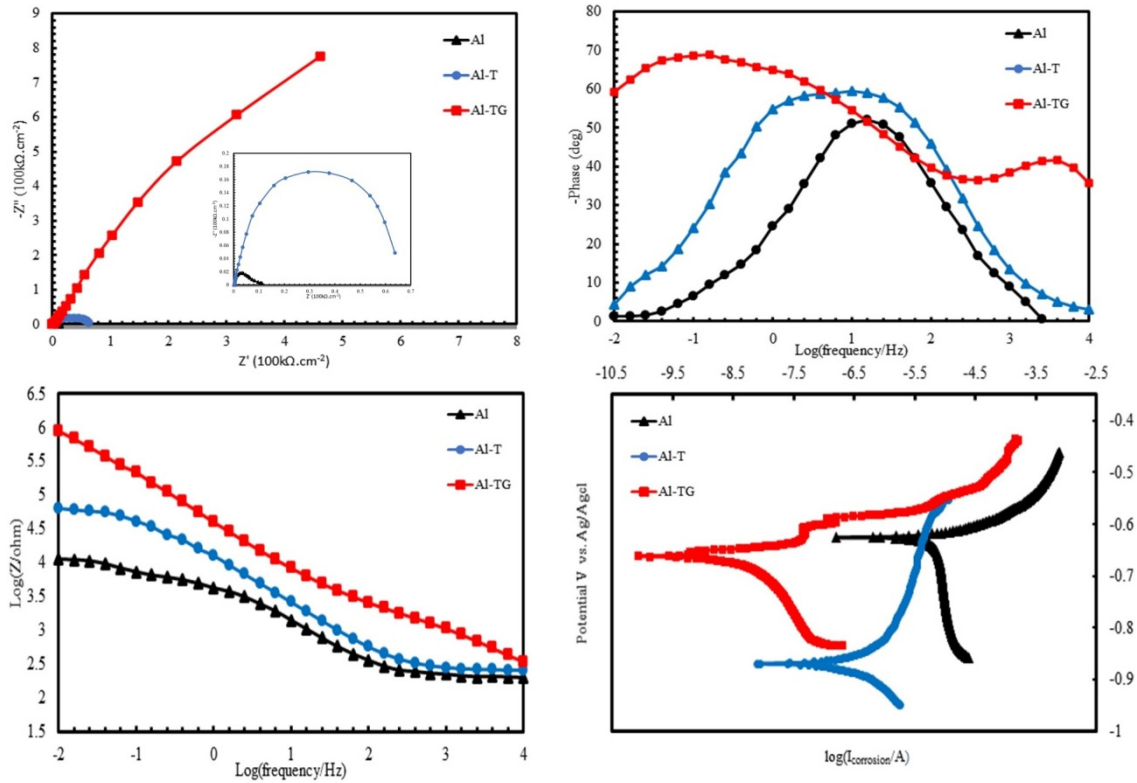


Fig. 5- Nyquist, bode, phase, and polarization curves of Al, Al-T, and Al-TG in 3.5% NaCl aqueous solution.

Table 3- corrosion speed and current density calculated from the polarization curve by Tafel extrapolation for Al, T, and S samples

Sample name	Corrosion Current Density(A/cm <sup>2</sup> )	Corrosion Speed (mm/year)
Al	$1.27 \times 10^{-5}$	$1.38 \times 10^{-1}$
Al-T	$3.57 \times 10^{-7}$	$3.86 \times 10^{-3}$
Al-TG	$4.58 \times 10^{-9}$	$4.95 \times 10^{-5}$

extrapolation was done on polarization curves. Table 3 shows corrosion speed and current density calculated from the polarization curve by Tafel extrapolation for Al, Al-T, and Al-TG samples. Results indicated that Al-T and Al-TG corrosion current density were  $3.57 \times 10^{-7}$  A/cm<sup>2</sup> and  $4.58 \times 10^{-9}$  A/cm<sup>2</sup>, respectively. In comparison with the bare Al substrate with  $1.27 \times 10^{-5}$  A/cm<sup>2</sup> corrosion current density, a noticeable improvement in corrosion resistance has been achieved by coating deposition. The corrosion speed reduced up to 2788 times for the Al-TG in comparison with bare Al.

As mentioned before, comparing Al, Al-T, and Al-TG with Etch, E-T, and E-TG is not possible due to the considerable difference in coating thickness, which will have a significant impact on EIS and polarization results. In addition to that, the same process was done for coating deposition on

all samples. So that one can compare the effect of substrate preparation on both corrosion resistance and WCA. On the same coating thickness, a hydrophobic coating should have higher corrosion resistance, but in different coating thicknesses, comparing corrosion resistance is not possible, and each set of samples should be compared in their own group. It is worth mentioning that a reduction in coating corrosion resistance in comparison with Al, Al-T, and Al-TG is incorrect due to two main reasons:

1- The apparent reason for this decrease in coating corrosion resistance in E-T and E-TG in comparison with Al-T and Al-TG is that the coating thickness is up to 4 times lower in E-T and E-TG samples which can drastically decrease coating corrosion resistance.

2- In order to measure corrosion current

density and in total corrosion behavior, a constant area of different samples is exposed to 3.5% NaCl solution. In fact, each sample has an apparent and real surface area and increasing the surface micro, and nanoscale roughness could lead to increase in real surface area in comparison with As mentioned earlier in order to increase WCA, chemical etching was used before coating deposition to increase surface micro and nanoscale roughness on the substrate; using the chemical etching had led to increase in real surface area in contact with 3.5% NaCl solution, while on Al, Al-T and Al-TG the real surface area and apparent area value are close.

In Fig. 6, results from EIS and polarization tests are shown. The Nyquist plot shows lower corrosion resistance in comparison to Al-T and Al-TG, but as mentioned before, this is due to lower coating

thickness and an increase in real area in contact with 3.5% NaCl. These two reasons will both highly reduce the coating corrosion resistance in comparison with Al-T and Al-TG. Hydrophobicity of E-T and E-TG samples indeed had a positive effect on increasing coating corrosion resistance, but this is not enough to compensate for the other two mentioned adverse effects. Table 4 shows corrosion speed and current density calculated from the polarization curve by Tafel extrapolation for Etch, E-T and E-TG samples. The results show that the corrosion speed of E-TG is about 4 times slower than the Etch sample and about 1.6 times lower than E-T. That is due to the uniformity of the TEOS/GPTMS hybrid sol-gel coating in comparison with the E-T sample, which has possible cracks or deficiencies in protecting the substrate.

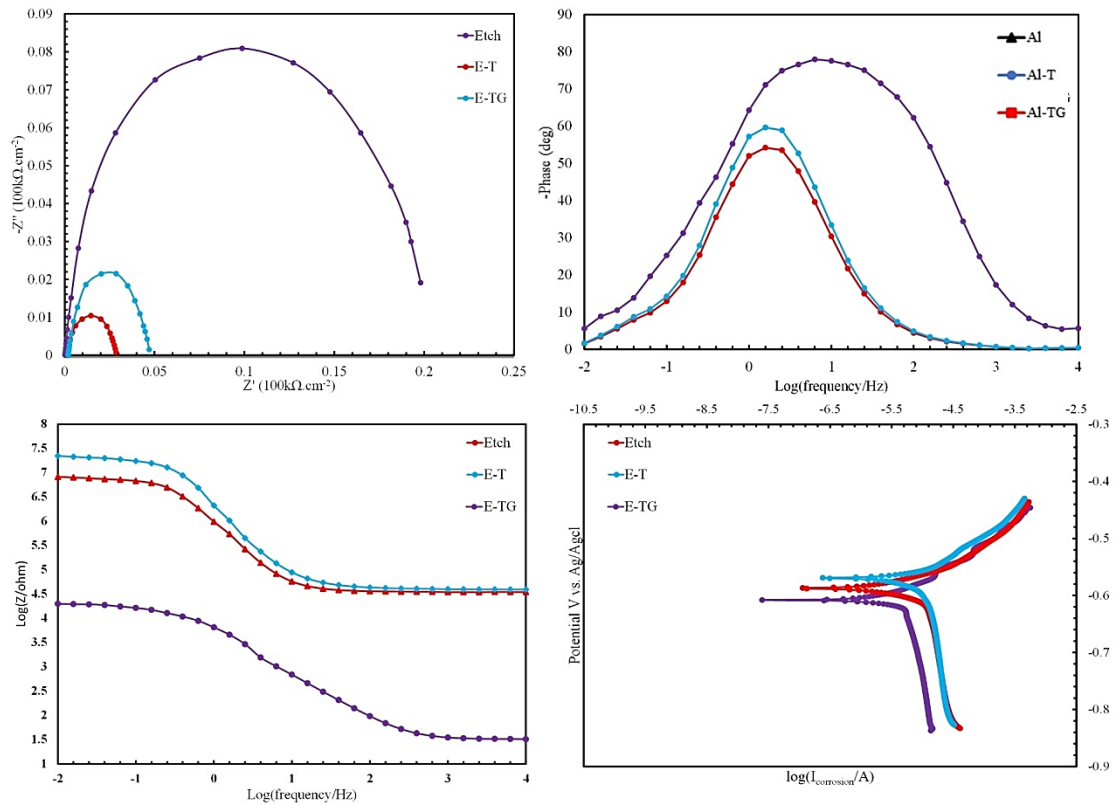


Fig. 6- Nyquist, bode, phase, and polarization curves of Etch, E-T and E-TG samples in 3.5% NaCl aqueous solution.

Table 4- corrosion rate and current density calculated from the polarization curve by Tafel extrapolation for Al, T, and S samples

Sample name	Corrosion Current Density(A/cm <sup>2</sup> )	Corrosion Rate (mm/year)
E	6.83×10 <sup>-6</sup>	7.39×10 <sup>-2</sup>
E-T	2.33 ×10 <sup>-6</sup>	2.53×10 <sup>-2</sup>
E-TG	1.45 ×10 <sup>-6</sup>	1.57×10 <sup>-2</sup>

#### 4. Conclusion

Hydrophobicity has been achieved without surface functionalization using a novel wet chemical etching route to modify surface roughness followed by a sol-gel coating. The WCA increased from 0° (Etch) to 118° (E-TG) on chemically etched substrate. FESEM and AFM were used to investigate the effect of surface roughness on WCA. In addition to that, EIS and polarization have been done to study the corrosion behavior. The corrosion resistance on E-T and E-TG is lower than Al-T and Al-TG samples. That is due to lower coating thickness (up to 4 times) on the etched substrate. The AFM and FESEM study of the coating substrate indicated that the coating followed the protrusion and bumps of the substrate affecting its final surface roughness. According to the Wenzel wetting model, the surface roughness has a relation with the WCA; in this case, the optimized roughness was achieved by deposition of hybrid sol-gel coating of the chemically etched substrate.

On the other hand, increasing the surface roughness in the micro and nanoscale by chemical etching will lead to an increase in real area in contact with 3.5% NaCl solution in comparison to the apparent area. Lower coating thickness and higher real surface area, are two main reasons for lower corrosion resistance. On the other hand, hydrophobicity of the coating should enhance the corrosion resistance. However, it is not enough to withstand the negative effect of the lower thickness and higher real surface area.

#### References

- Ganesh VA, Raut HK, Nair AS, Ramakrishna S. A review on self-cleaning coatings. *Journal of Materials Chemistry*. 2011;21(41):16304.
- Dalawai SP, Saad Aly MA, Latthe SS, Xing R, Sutar RS, Nagappan S, et al. Recent Advances in durability of superhydrophobic self-cleaning technology: A critical review. *Progress in Organic Coatings*. 2020;138:105381.
- Mohamed AMA, Abdullah AM, Younan NA. Corrosion behavior of superhydrophobic surfaces: A review. *Arabian Journal of Chemistry*. 2015;8(6):749-65.
- Al-Naamani L, Dobretsov S, Dutta J, Burgess JG. Chitosan-zinc oxide nanocomposite coatings for the prevention of marine biofouling. *Chemosphere*. 2017;168:408-17.
- Kazem HA, Chaichan MT, Al-Waeli AHA, Sopian K. A review of dust accumulation and cleaning methods for solar photovoltaic systems. *Journal of Cleaner Production*. 2020;276:123187.
- E J, Jin Y, Deng Y, Zuo W, Zhao X, Han D, et al. Wetting Models and Working Mechanisms of Typical Surfaces Existing in Nature and Their Application on Superhydrophobic Surfaces: A Review. *Advanced Materials Interfaces*. 2017;5(1):1701052.
- Dai X, Stogin BB, Yang S, Wong T-S. Slippery Wenzel State. *ACS Nano*. 2015;9(9):9260-7.
- Kwon Y, Patankar N, Choi J, Lee J. Design of Surface Hierarchy for Extreme Hydrophobicity. *Langmuir*. 2009;25(11):6129-36.
- Lai Y, Huang Y, Wang H, Huang J, Chen Z, Lin C. Selective formation of ordered arrays of octacalcium phosphate ribbons on TiO<sub>2</sub> nanotube surface by template-assisted electrodeposition. *Colloids and Surfaces B: Biointerfaces*. 2010;76(1):117-22.
- Song J, Xu W, Liu X, Lu Y, Wei Z, Wu L. Ultrafast fabrication of rough structures required by superhydrophobic surfaces on Al substrates using an immersion method. *Chemical Engineering Journal*. 2012;211-212:143-52.
- Borras A, Barranco A, González-Elipse AnR. Reversible Superhydrophobic to Superhydrophilic Conversion of Ag@TiO<sub>2</sub> Composite Nanofiber Surfaces. *Langmuir*. 2008;24(15):8021-6.
- Bravo J, Zhai L, Wu Z, Cohen RE, Rubner MF. Transparent Superhydrophobic Films Based on Silica Nanoparticles. *Langmuir*. 2007;23(13):7293-8.
- Sun C, Ge L-Q, Gu Z-Z. Fabrication of super-hydrophobic film with dual-size roughness by silica sphere assembly. *Thin Solid Films*. 2007;515(11):4686-90.
- Ma M, Hill RM, Lowery JL, Fridrikh SV, Rutledge GC. Electrospun Poly(Styrene-block-dimethylsiloxane) Block Copolymer Fibers Exhibiting Superhydrophobicity. *Langmuir*. 2005;21(12):5549-54.
- Mizukoshi T, Matsumoto H, Minagawa M, Tanioka A. Control over wettability of textured surfaces by electrospray deposition. *Journal of Applied Polymer Science*. 2006;103(6):3811-7.
- Guglielmi M. Sol-gel coatings on metals. *Journal of Sol-Gel Science and Technology*. 1997;8(1-3):443-9.
- Khramov AN, Voevodin NN, Balyshev VN, Donley MS. Hybrid organo-ceramic corrosion protection coatings with encapsulated organic corrosion inhibitors. *Thin Solid Films*. 2004;447-448:549-57.
- Pepe A, Aparicio M, Durán A, Ceré S. Cerium hybrid silica coatings on stainless steel AISI 304 substrate. *Journal of Sol-Gel Science and Technology*. 2006;39(2):131-8.
- G. KICKELBICK, *Hybrid materials: synthesis, characterization, and applications*: John Wiley & Sons, 2007.
- Hojjati Najafabadi A, Shoja Razavi R, Mozaffarinia R, Rahimi H. A New Approach of Improving Rain Erosion Resistance of Nanocomposite Sol-Gel Coatings by Optimization Process Factors. *Metallurgical and Materials Transactions A*. 2014;45(5):2522-31.